Near micron-sized cirrus cloud particles in high-resolution infrared spectra: An orographic case study

Brian H. Kahn,[1] Annmarie Eldering,[1,2] Shepard A. Clough,[3] Eric J. Fetzer,[2] Evan Fishbein,[2] Michael R. Gunson,[2] Sung-Yung Lee,[2] Peter F. Lester,[4] and Vincent J. Realmuto[2]

Received 10 January 2003; revised 3 March 2003; accepted 17 March 2003; published 29 April 2003.

[1] The high-resolution spectra of the Atmospheric Infrared Sounder (AIRS) provide a global view of small-particle-dominated cirrus clouds, and they exist over much larger spatial extents than seen in previous aircraft campaigns. As shown by simulations using a plane-parallel scattering radiative transfer (RT) model and realistic ice particle shapes, the shape of the radiance spectra in the atmospheric windows is uniquely influenced by small ice crystals. Minima in the brightness temperature (BT) spectra between 800 to 850 cm^{-1} are seen for ice particles smaller than 3 μm in the RT simulations and AIRS spectra. A case study of an orographic cirrus cloud observed on October 2, 2002, over the central Andes of South America is presented with spectral BT differences up to 63K between 998 and 811 cm^{-1}. *INDEX TERMS:* 0305 Atmospheric Composition and Structure: Aerosols and particles (0345, 4801); 0320 Atmospheric Composition and Structure: Cloud physics and chemistry; 0360 Atmospheric Composition and Structure: Transmission and scattering of radiation; 3359 Meteorology and Atmospheric Dynamics: Radiative processes; 3360 Meteorology and Atmospheric Dynamics: Remote sensing. **Citation:** Kahn, B. H., A. Eldering, S. A. Clough, E. J. Fetzer, E. Fishbein, M. R. Gunson, S.-Y. Lee, P. F. Lester, and V. J. Realmuto, Near micron-sized cirrus cloud particles in high-resolution infrared spectra: An orographic case study, *Geophys. Res. Lett.*, *30*(8), 1441, doi:10.1029/2003GL016909, 2003.

1. Introduction

[2] The characterization of the effect of small ice particles on cirrus cloud optical properties is one of the outstanding problems in cloud research and necessitates better observations of the smallest particles [*Lynch et al.*, 2002]. Ice crystals, water droplets, and aerosols have broad extinction features (10's to 100's of wave numbers wide) in the infrared with sensitivity to effective radii (r_{eff}), optical thickness (τ), and cloud altitude. Top-of-atmosphere (TOA) radiative forcing is highly sensitive to τ and r_{eff} [*Fu and Liou*, 1993], with small-particle ice clouds producing negative TOA radiative forcing at lower IWP than large-particle ice clouds. Previous work has focused on determining approximate values of r_{eff} for cirrus clouds, with greater sensitivity for moderate τ and small effective radii [*Ackerman et al.*, 1995]. *Smith et al.* [1998] discuss an example of a ice cloud containing small particles observed by the High-resolution Interferometer Sounder flown on the NASA ER-2 during the Subsonic Aircraft Contrail and Cloud Effects Special Study. An r_{eff} of 7 μm is derived by *Smith et al.* [1998] by fitting the spectral shape of the cloud emissivity in the 750–1000 cm^{-1} atmospheric window using a radiative transfer model with ice spheres.

[3] The Atmospheric Infrared Sounder (AIRS) on the EOS-Aqua platform is a high-resolution ($\nu/\Delta\nu$ = 1200) grating spectrometer that scans at angles of ±49.5° from nadir, at both visible and infrared wavelengths. The infrared spectral coverage covers three bands in the 3.7–15.4 μm range (649–1136, 1265–1629, and 2169–2674 cm^{-1}), with a surface footprint of 13.5 km diameter at nadir view [*Aumann and Pagano*, 1994]. The entire 750–1000 cm^{-1} atmospheric window is covered by AIRS, although the spectral coverage of the 1050–1250 cm^{-1} window is not complete. This window region is examined in the current study. Daytime observations lead to a large reflected solar component in the 2400–2650 cm^{-1} atmospheric window and are thus not used for this analysis.

[4] We simulate TOA brightness temperature (BT) spectra for small ice particles with the Code for High-resolution Accelerated Radiative Transfer with Scattering (CHARTS), a plane-parallel monochromatic radiative transfer model with multiple scattering [*Moncet and Clough*, 1997] in conjunction with the Line By Line Radiative Transfer Model (LBLRTM). The single scattering parameters for the ice particles are calculated using the *T*-matrix method [*Mishchenko and Travis*, 1998]. Previous work using radiative transfer models to simulate a small set of TOA BT spectra for particles larger than 4.5 μm [*Bantges et al.*, 1999; *Chung et al.*, 2000] produced spectral shapes in the atmospheric windows much like those shown below. *Prabhakara et al.* [1990] show examples of IR spectra from the Infrared Interferometer Spectrometer (IRIS) in polar regions which resemble modeled spectra for ice clouds with r_{eff} larger than 3–4 μm.

2. Model Results

[5] Figure 1a shows the variations in simulated TOA BT spectra for a range of r_{eff} at a fixed 950 cm^{-1} optical depth of 0.82. Figure 1b shows the variation in simulated TOA BT spectra for a range of τ at a fixed particle effective radius of 2 μm. The simulated spectra are calculated using a vertical

[1]Department of Atmospheric Sciences, University of California at Los Angeles, Los Angeles, CA, USA.
[2]Jet Propulsion Laboratory, Pasadena, CA, USA.
[3]Atmospheric and Environmental Research, Inc., Cambridge, MA, USA.
[4]Department of Meteorology, San Jose State University, San Jose, CA, USA.

0094-8276/03/2003GL016909$05.00

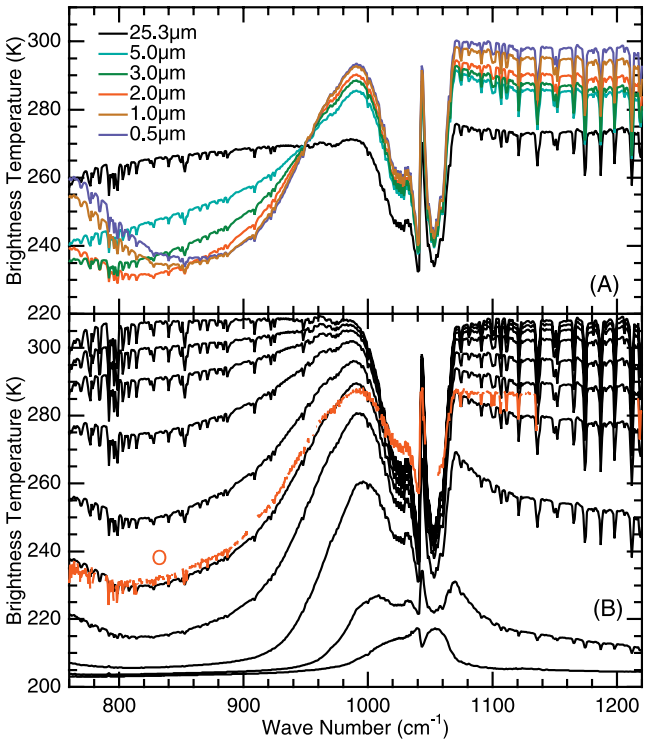

Figure 1. Simulated TOA BT spectra using CHARTS and monodisperse cylindrical ice particles. (a) An assortment of r_{eff} at an optical depth (τ) of 0.82 at 950 cm^{-1}. (b) TOA BT spectra for 2 μm particles across a realistic range of τ at 950 cm^{-1} (τ = .0133, .0664, .133, .265, .531, .854, 1.33, 2.65, 6.64, and 13.3) with τ increasing downward (colder BT spectra). AIRS spectrum O from Figure 2 is superimposed for reference.

profile of T and H_2O taken from the NCEP AVN model at 24°S 64°W at 1800 UTC, just to the east of the northern Argentinian Andes. A total of 43 levels from the surface to 90 km are used, and the model clouds are constrained to 12–13 km heights. Monodisperse cylindrical ice particles with aspect ratios of unity are used for all simulations. We have explored the effects of particle shapes using cylinders, spheroids [*Mishchenko and Travis*, 1998], and hexagonal cylinders [*Baran et al.*, 2002] for particles smaller than 3 μm and all particle shapes produce very similar extinction spectral shapes. Spectral shape results because the real part of the index of refraction tends to a minimum near 950 cm^{-1} resulting in reduced extinction for small ice particles [*Arnott et al.*, 1995]. We use the water ice index of refraction from *Toon et al.* [1994] measured at 163K. Comparisons are made with *Clapp et al.* [1995] refractive indices at temperatures ranging from 160 K to 210 K, and BT sensitivity up to 1–3 K (5 K) is noted in the 750–1000 (1050–1250) cm^{-1} windows, especially near the BT minima and maxima. As seen in Figure 1a, the extinction for particle sizes of 25.3 μm is nearly constant in the window regions. Greater spectral distortion occurs for smaller particles. For a particle size of 3 μm in Figure 1a, a broad minimum at 800 cm^{-1} appears, with decreasing BT from 750 to 800 cm^{-1} and strongly increasing from 800 to 1000 cm^{-1}. At 2 μm the minimum is smaller relative to 750 cm^{-1} and the minimum shifts from 800 to 820 cm^{-1}. Similarly, for 0.5 μm size particles the minimum is more pronounced and shifts to 860 cm^{-1}. The spectral distortion of increasing τ for the smaller particle size of 2 μm is shown in Figure 1b. This distortion is also a function of the vertical temperature profile, and atmospheres with larger tropopause to surface temperature differences will show greater distortion.

3. Observations

[6] AIRS spectra with spectral dependencies similar to those modeled have been observed in cirrus intermittently between July and December 2002 at all latitudes in and around orography, convection, midlatitude and tropical cyclones, and elsewhere. As an example, we present an orographic cirrus case for October 2, 2002, at 1800 UTC centered near 24°S 64°W in northern Argentina. The AIRS BT spectra for selected portions of this scene are shown in Figure 2. The location of each spectrum is noted on Figure 3b. The average NEdT (noise equivalent delta temperature) across the selected channels is 0.32 K. The strong observed spectral dependencies can be explained by very small ice particles along with a warm surface and cold tropopause. The NCEP AVN vertical T and H_2O profile used in the simulation shows the 1000 mb level and tropopause temperatures to be, respectively, 310.6 K and 195.2 K. Spectrum S has the largest BT difference (63 K) between 998 and 811 cm^{-1}. Notice the BT minima in the spectra near 800 cm^{-1} for A, B, C, O, and S. In simulations this shape is produced only by a preponderance of small particles of roughly 3 μm radius or smaller. Other spectra such as

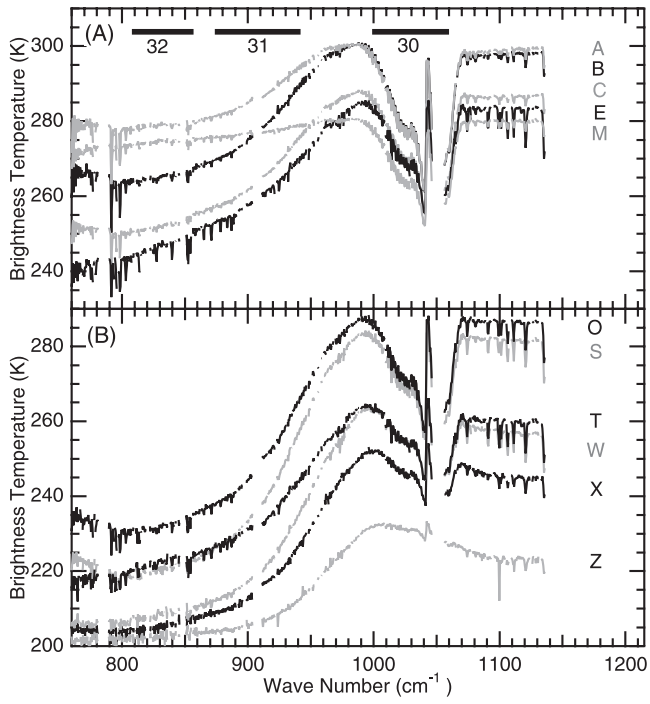

Figure 2. Selected AIRS spectra with locations shown in Figure 3b. (a) Spectra at warmer temperatures which indicate thinner clouds. (b) Spectra at colder temperatures which indicate thicker clouds. MODIS channels 30, 31, and 32 for a spectral response function of 0.05 and greater shown for reference.

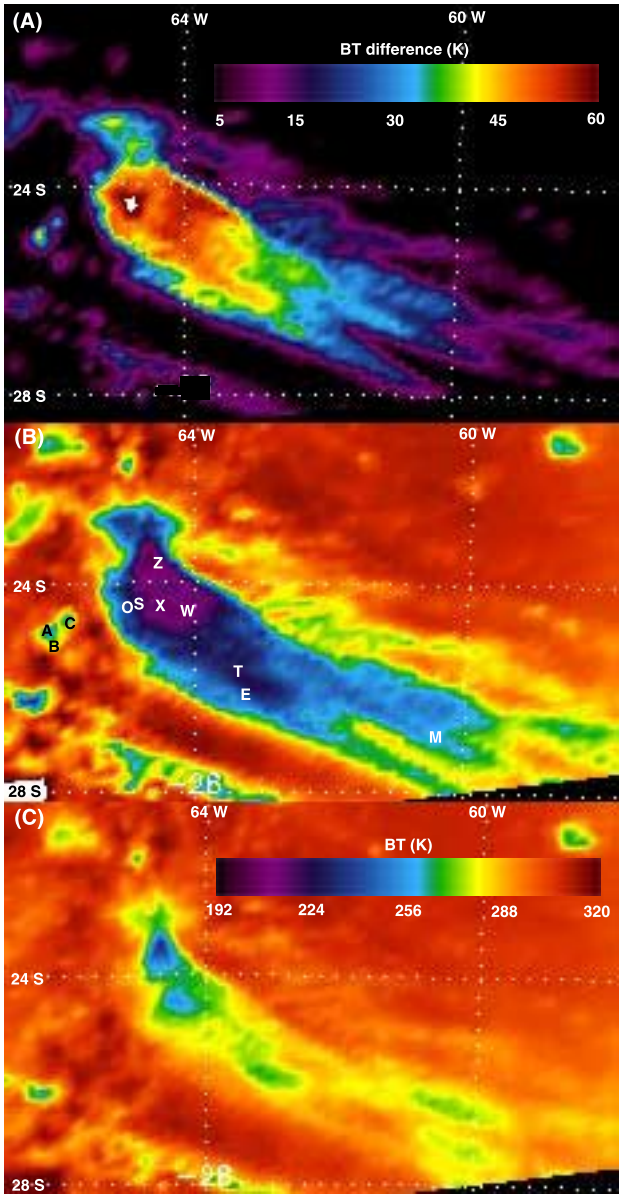

Figure 3. AIRS BT maps for granule 180, October 2nd, 2002, at 1800 UTC. (a) Difference of BT at 998 and 811 cm^{-1}. (b) BT map for 811 cm^{-1}, with letters denoting locations of selected AIRS spectra shown in Figure 2. (c) BT map for 998 cm^{-1}.

E and T display strong spectral variation without BT minima, indicating the r_{eff} is somewhat larger. In contrast spectrum M is quite flat with rather low BTs, indicating larger particle sizes in the downwind portion of the cloud.

[7] We now turn to the larger context and consider the plausibility of the presence of such small ice crystals. Figure 3 shows BT maps in and around the ice clouds of small particles. Panel (a) is the difference between panels (b) (998 cm^{-1}) and (c) (811 cm^{-1}). Notice the WNW-ESE oriented cirrus band and adjacent patches of cloud to the west. Inspection of GOES-8 imagery (not shown) indicates that these cloud features are orographically induced; i.e., they are stationary for at least six hours ±1800 UTC [*Scorer*, 1986]. Examination of Figure 3a indicates that the largest spectral BT differences are located at the upwind portion of the cirrus band and in the isolated clouds over the Andes. The spectral BT differences are reduced farther downwind, evidently caused by a combination of optically thinner cloud and larger particle size.

[8] Coincident Moderate Resolution Imaging Spectrometer (MODIS) [*King et al.*, 1992] Aqua imagery is shown in Figure 4a for the BT difference between channels 31 (centered at 910 cm^{-1}) and 32 (centered at 830 cm^{-1}). The high spatial resolution of MODIS is apparent in Figure 4, and the low spectral resolution as compared against AIRS is illustrated in Figure 2. The broad cirrus band has a distinct edge paralleling the crest of the Andes as seen in the MODIS RGB VIS image in Figure 4b. In addition to patchy wave clouds over the mountains, rows of narrow cloud bands are also visible east of, and parallel to, the Andes. Further evidence supporting significant lee wave activity is found in the presence of strong, stable westerly flow as documented by available upper air analysis charts and the Antofagasta radiosonde (not shown). The maximum spectral BT difference noted in Figure 4a is about 19 K, located near the western and northeastern edges of the orographic cirrus band, and near the centers of the isolated wave clouds just to the west. In Figure 3a the largest AIRS spectral BT difference (63 K) is observed in the orographic cirrus band, with approximately half that value in the isolated wave clouds. This demonstrates the tradeoff between spectral resolution and spatial resolution. AIRS shows more drastic BT changes across the spectra but are representative of a 13.5 km footprint. The high spatial resolution of MODIS resolves smaller cloud features

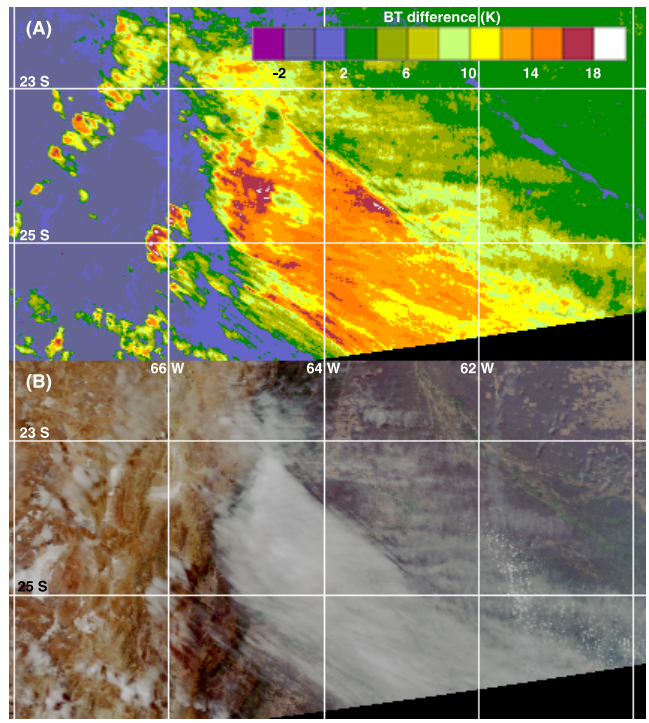

Figure 4. (a) Coincident MODIS-Aqua BT difference between channels 31 and 32 (centered at 910 and 830 cm^{-1}, respectively) for a subset of the scene in Figure 3. (b) RGB combination of MODIS VIS channels.

but cannot resolve the spectral dependence in the atmospheric window.

4. Discussion

[9] *In situ* observations of ice crystal size and number concentration in wave clouds taken by *Heymsfield and Miloshevich* [1995] show the existence of large numbers of particles smaller than 3 μm. Size distributions were reported for aircraft flight segments approximately 0.2 km long or less. Many size distributions show a large particle mode, but over some flight segments (1 km long or less) the smaller mode is dominant. Thus the results here are consistent with known microphysical properties of some wave clouds. Additionally, strong spectral dependence in radiance results from the emissivity of some land surfaces [*Rees*, 2001]. However, AIRS spectra in clear scenes over the geographic region studied here do not resemble small particle spectra.

[10] Multi-spectral techniques such as the split-window [e.g., *Inoue*, 1985] and tri-spectral [*Strabala et al.*, 1994] approaches have proven to be useful for identifying cirrus clouds. These techniques utilize channels in the atmospheric windows to discern different cloud types and values of r_{eff}. When r_{eff} becomes smaller than 10 μm or so, the spectral variation in the 750–1000 cm^{-1} window more strongly distorts from a straight line, and develops a minimum in the radiance spectra near 800 cm^{-1} (see Figure 1a). In order to retrieve accurate values of r_{eff} for small particles an IR emission instrument must have enough channels across the windows to resolve details of the spectral dependence. For r_{eff} larger than 10 μm this is done with only 2 or 3 channels; however more channels are needed as particle size is reduced. High spectral resolution IR instruments will lead to accurate retrievals of r_{eff} for small particle sizes because the spectral dependence is very sensitive to size changes smaller than 10 μm, according to model calculations.

5. Conclusions

[11] AIRS spectra containing unique spectral signatures consistent with small ice particles are presented. Only simulations that include ice particles with a radius of 3 μm or smaller can reproduce the observed spectral dependence in the atmospheric windows. When equal numbers of small and large particles are modeled as a distribution, the simulated extinction spectrum is very similar to that of the large particles alone. Thus the observed signatures presented here are indicative of a distribution dominated by a small particle mode. Although the AIRS footprint of 13.5 km is large compared to the scale of cloud structure as seen in MODIS, AIRS has shown that small ice particle clouds do exist on this spatial scale. In the future, similar high spectral resolution instruments such as TES with higher spatial (5 × 7 km) resolution [*Beer et al.*, 2001] will see even smaller cloud features.

[12] **Acknowledgments.** The authors thank Moustafa Chahine, Michael King, and the AIRS and MODIS science teams for making their data available for this work. The authors thank Roger Davies, Barney Farmer, Michael Garay, Andrew Heymsfield, Bill Irion, Kuo Nan Liou, and Michael Mishchenko for useful conversations, and two anonymous reviewers for improvements to the manuscript. This work was funded by the Caltech President's Fund (AE and BHK) and NASA-ESS fellowship NGT-5-30372 (BHK). A portion of this work was performed at the Jet Propulsion Laboratory, California Institute of Technology, under contract with NASA.

References

Ackerman, S. A., W. L. Smith, A. D. Collard, X. L. Ma, H. E. Revercomb, and R. O. Knuteson, Cirrus cloud properties derived from high spectral resolution infrared spectrometry during FIRE II. Part II: Aircraft HIS results, *J. Atmos. Sci.*, *52*, 4246–4263, 1995.

Arnott, W. P., Y. Y. Dong, and J. Hallett, Extinction efficiency in the infrared (2–18 μm) of laboratory ice clouds: Observations of scattering minima in the Christiansen bands of ice, *Appl. Opt.*, *34*, 541–551, 1995.

Aumann, H. H., and R. J. Pagano, Atmospheric Infrared Sounder on the Earth Observing System, *Opt. Eng.*, *33*, 776–784, 1994.

Bantges, R. J., J. E. Russell, and J. D. Haigh, Cirrus cloud top-of-atmosphere radiance spectra in the thermal infrared, *J. Quant. Spectrosc. Radiat. Transfer*, *63*, 487–498, 1999.

Baran, A. J., S. Havemann, and D. Mackowski, A database of hexagonal column optical properties for wavelengths ranging between 0.2 μm to 30 μm produced for ANNEX 7, Contract no. 4b/3/02, DEFRA UK, 2002.

Beer, R., T. A. Glavich, and D. M. Rider, Tropospheric emission spectrometer for the Earth Observing System's Aura satellite, *Appl. Opt*, *40*, 2356–2367, 2001.

Chung, S., S. Ackerman, and F. van Delst, Model calculations and interferometer measurements of ice-cloud characteristics, *J. Appl. Meteor.*, *39*, 634–644, 2000.

Clapp, M. L., R. E. Miller, and D. R. Worsnop, Frequency-dependent optical constants of water ice obtained directly from aerosol extinction spectra, *J. Phys. Chem.*, *99*, 6317–6326, 1995.

Fu, Q., and K. N. Liou, Parameterization of the radiative properties of cirrus clouds, *J. Atmos. Sci.*, *50*, 2008–2025, 1993.

Heymsfield, A. J., and L. M. Miloshevich, Relative humidity and temperature influences on cirrus formation and evolution: Observations from wave clouds and FIRE II, *J. Atmos. Sci.*, *52*, 4302–4326, 1995.

Inoue, T., On the temperature and effective emissivity determination of semi-transparent cirrus clouds by bi-spectral measurements in the 10 μm window region, *J. Meteor. Soc. Japan*, *63*, 88–98, 1985.

King, M. D., Y. J. Kaufman, W. P. Menzel, and D. Tanré, Remote sensing of cloud, aerosol, and water vapor properties from the Moderate Resolution Imaging Spectrometer (MODIS), *IEEE Trans. Geosci. Remote Sens.*, *30*, 2–27, 1992.

Lynch, D. K., K. Sassen, A. Del Genio, A. J. Heymsfield, P. R. Minnis, C. M. R. Platt, M. Quante, U. Schumann, and H. Sundqvist, Cirrus: The future, in *Cirrus*, edited by D. K. Lynch, K. Sassen, D. O'C. Starr, and G. L. Stephens, Oxford Press, New York, 449–455, 2002.

Mishchenko, M. I., and L. D. Travis, Capabilities and limitations of a current Fortran implementation of the *T*-matrix method for randomly oriented, rotationally symmetric scatterers, *J. Quant. Spectrosc. Radiat. Transfer*, *60*, 309–324, 1998.

Moncet, J. L., and S. A. Clough, Accelerated monochromatic radiative transfer for scattering atmospheres: Application of a new model to spectral radiance observations, *J. Geophys. Res.*, *102*, 21,853–21,866, 1997.

Prabhakara, C., J.-M. Yoo, G. Dalu, and R. S. Fraser, Deep optically thin cirrus clouds in the polar regions. Part I: Infrared extinction characteristics, *J. Appl. Meteor.*, *29*, 1313–1329, 1990.

Rees, W. G., *Physical Principles of Remote Sensing*, Cambridge Univ. Press, Cambridge, United Kingdom, 2001.

Scorer, R. S., *Cloud Investigation by Satellite*, John Wiley and Sons, New York, 1986.

Smith, W. L., S. Ackerman, H. Revercomb, H. Huang, D. H. DeSlover, W. Feltz, L. Gumley, and A. Collard, Infrared spectral absorption of nearly invisible cirrus clouds, *Geophys. Res. Lett.*, *25*, 1137–1140, 1998.

Strabala, K. I., S. A. Ackerman, and W. P. Menzel, Cloud properties inferred from 8–12 μm data, *J. Appl. Meteor.*, *33*, 212–229, 1994.

Toon, O. B., M. A. Tolbert, B. G. Koehler, A. M. Middlebrook, and J. Jordan, Infrared optical constants of H_2O ice, amorphous nitric acid solutions, and nitric acid hydrates, *J. Geophys. Res.*, *99*, 25,631–25,654, 1994.

B. H. Kahn and A. Eldering, Department of Atmospheric Sciences, UCLA, Los Angeles, CA 90095-1565, USA. (kahn@atmos.ucla.edu)

S. A. Clough, Atmospheric and Environmental Research, Inc., Cambridge, MA 02139, USA.

A. Eldering, E. J. Fetzer, E. Fishbein, M. R. Gunson, S.-Y. Lee, and V. J. Realmuto, Jet Propulsion Laboratory, California Institute of Technology, Pasadena, CA 91109-8001, USA.

P. F. Lester, Department of Meteorology, SJSU, San Jose, CA 95192, USA.